Photoactivity of CdS Particles Grown in Pt-loaded Zeolite Y

Young-Ju Hwang, Sung-Jin Kim,* Sejin Park,† Jae-Hun Yang,† Hasuck Kim,† and Jin-Ho Choy†

Department of Chemistry, Ewha Womans University, Seoul 120-750, Korea
†Department of Chemistry and Center for Molecular Catalysis, Seoul National University, Seoul 151-742, Korea
Received October 26, 1999

An integrated photocatalyst was prepared and its photoelectrocatalytic behavior for solar energy conversion was investigated. To make an integrated photocatalyst for hydrogen evolution, Pt and CdS clusters were embedded in zeolite as a cocatalyst and a photocatalyst, respectively. Pt particles were embedded in zeolite Y by ion exchange reaction with Pt $(NH_3)_4^{2+}$ and activation and reduction processes were followed. CdS clusters in zeolite Y cages were prepared by ion exchange reaction with Cd^{2+} and sulfurization with Na_2S in aqueous solution was followed. The existence of CdS clusters in the cavities of zeolite Y was detected by IR spectra. UV absorption edges of the samples prepared show blue shifts about 0.03-0.12 eV from the edge of bulk CdS, which is an indication of CdS clusters formed in zeolite Y. The pore structure of samples was analyzed by BET and Langmuir method. The solar energy conversion into hydrogen was investigated, where sodium tartrate solution was used as a hole scavenger. We could observe that 1 wt% Pt supported sample was the most effective photocatalyst for hydrogen evolution (62 μL/mg after 4 hour reaction).

Introduction

Photocatalytic hydrogen evolution with semiconductor particles has attracted much attention due to their potential use for solar energy conversion process. Electron transfer reaction in the hydrogen evolution can be induced by the photoexcitation of inorganic semiconductor materials.[1] Researches during the past decade have suggested that the photocatalytic redox processes of converting low-energy starting materials, such as H_2O, to high-energy product mixtures, such as H_2+1/$2O_2$, are important for potential applications.[2]

Even though, there are still problems to overcome in the semiconductor photoelectrodes, some inorganic semiconductors are known to be the most efficient photocatalytic materials for photo-electrochemical cells.[1] As far as the band gap (E_g) of the semiconductor is concerned, the optimum band gap for the maximum efficiency of the photoelectrochemical cell is considered to be about 1.4 eV.[3] However, the value of E_g is not the only criterion in selecting a semiconductor photoelectrode for the generation of chemical fuel or electricity.

One of problems in the semiconductors for the conversion of solar power is the back reaction of energetic redox products at the semiconductor/liquid electrolyte interface. To obtain a thermodynamically favorable condition for desired photocatalytic redox process, E_B must be as close as possible to E_g in its magnitude. Here, E_B is the difference between E_{redox}, the electrochemical potential of the solution, and E_{CB} (the energy of the conduction band for n-type semiconductor) or E_{VB} (the energy of the valence band for p-type semiconductors), and E_{redox} is associated with half-cell reaction occurring at the photoelectrode.[4]

For practical applications of the desired photoinduced redox reaction of the materials, it is important to consider their stability and selectivity under various conditions. Considering band gap and solar response along with stability in solution, a semiconducting transition metal chalcogenide CdS has been considered to be a suitable material.[5]

Recently, many efforts have been made to study the photoactive small-particles due to their large surface areas and a variety of new interesting properties as a catalyst.[6-18] In terms of size-controllability and stability as a supporting matrix, zeolites are alternative candidates for supporting these photoactive species.[19] Their aluminosilicate frameworks render them high stability under ambient conditions, and their various structural porosity allows controlled variances in hosting and growing of particles.[20-27]

In our work, integrated photocatalyst, CdS and Pt embedded zeolite-Y were constructed under various conditions. The factors affecting catalytic efficiencies of differently prepared catalysts were investigated.

Experimental Section

Zeolite Na-Y is the synthetic counterpart of the natural occurring mineral faujasite.[29-31] As shown in Figure 1, zeolite has 13 Å tetrahedral symmetry cages (α or supercage), sodalite cages (tetradecahedron with 14 vertices with 2.3 Å opening) and 3 Å double six-membered rings (hexagonal prism) between two sodalite cages. The chemical composition of zeolite Na-Y used in this study was $Na_{58}[Al_{58}Si_{134}O_{384}]\cdot 240H_2O$ (Union Carbide). The Pt supported zeolite Y was prepared following the similar procedure of previous reports.[20-27] First, Na cations in zeolite Y were exchanged with Pt^{2+} by mixing zeolite powder and a 5×10^{-5}~3×10^{-4} mol/dm^{-3} aqueous solution of tetraamineplatinumnitrate, [Pt $(NH_3)_4$ $(NO_3)_2$] (99%, Strem Chemicals). The volume of solution to the weight of zeolite in the mixture was 100 mL: 1 g. The exchanged zeolite was then filtered, washed with

*Authors to whom correspondence should be addressed. Tel: +82-2-3277-2350, Fax: +82-2-3277-2384, E-mail: sjkim@mm.ewha.ac.kr

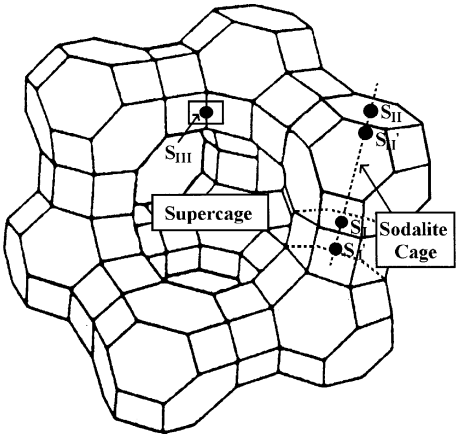

Figure 1. Zeolite Y supercage structure showing selected cation sites.

distilled water and dried in a vacuum oven at 300-320 K. The dried product was then activated by heating it under O_2 atmosphere and subsequently under H_2 flow at 573 K for 2 h. To obtain a uniform distribution of Pt in zeolite, the ion exchange reaction and reduction procedures were repeated several times. To investigate the effect of Pt on photocatalytic system, three samples, sample A, B, and C, were prepared with different Pt quantities and different preparation procedures. Sample A and B are prepared by adding different amounts of Pt quantities in each consecutive reaction step. The total amount of Pt intended to embed was 10 wt % for both sample A and B and 1 wt % for sample C. The amounts of Pt loaded at each reaction step for sample A were 0.003 g, 0.007 g, 0.015 g ,0.02 g, 0.025 g and 0.03 g. For sample B, 0.02 g of Pt was loaded in each step for five times. For sample C, 0.003 g of Pt at every step was loaded for five times.

For the formation of CdS clusters in the Pt-supported zeolite, the Pt-supported zeolite powder (~5 g) was slurried in distilled water with pH adjusted to 5.0 with nitric acid (Duksan Pure Chemicals Co., Ltd.). The cadmium nitrate ($Cd(NO_3)_2 \cdot 4H_2O$, 0.5 M, ~25 mL, Yoneyama Chemical Industries, Ltd.) was added into the slurry and the mixture was stirred at room temperature for 20 h. The zeolite powder with Cd^{2+} ion was collected by filtration, and washed extensively with distilled water. This filtered powder was dried in a vacuum oven at 300-320 K for 20 h and sulfurization was carried out by mixing and stirring this Cd^{2+} ion exchanged zeolite in Na_2S (0.1 M) solution. The mixture was stirred at room temperature for 20 h and precipitate was collected again by filtration and then extensively washed. Finally, the samples were dried at 300-320 K in a vacuum oven for 20 h. For comparison, we made CdS embedded zeolite without Pt supporting by using various sulfurization agents such as H_2S, Na_2S and thiourea (Hereafter, the three samples are referred to CdS-H_2S, CdS-Na_2S and CdS-thiourea, respectively).

The diffuse reflectance UV-vis. spectra of the colored samples were obtained with a Shimadzu UV-3101 with an integrating sphere. The absolute absorption coefficient of these semiconductor clusters was obtained by the diffuse reflectance equation of Kubelka-Munk (K-M),[28]

$$\alpha = S\,F(R) / 2\nu_P, \quad (1)$$

where α is the absorption coefficient (in units of 1/cm, normalized to the volume fraction of the semiconductor), S is the scattering coefficient and ν_P is the volume fraction of the semiconductor. F(R) is the K-M function defined as

$$F(R) = 1 - R^2 / 2R, \quad (2)$$

where R is the experimentally measured diffuse reflectance.

The IR spectra of bulk CdS, zeolite embedded CdS (CdS-H_2S and CdS-Na_2S), sample A, sample C and pristine zeolite were obtained in the range of 4000-400 cm^{-1} using a Perkin-Elmer 16F PCFT-IR. The change in crystallinity of the samples was analyzed by X-ray diffraction technique, using a Siemens D-500 diffractometer monitored at 40 kV and 20 mA, with Cu-Kα radiation (λ = 1.5408 Å) at a scan speed of 1 degree min^{-1} (in 2θ). The quantities of Cd and Pt embedded in zeolite were analyzed with an ICP-AES (Plasmascan 8410, Labtom Co).

The hydrogen evolution reaction was carried out in a reaction chamber as shown in Figure 2. An 8-mL of sodium tartrate aqueous solution adjusted to pH 4.1 with HCl was mixed with 2 mg of photocatalyst in the reaction chamber and was purged with N_2 gas. The light source was 1000W Xe lamp (Oriel) operated at 600 W. The light was collimated and passed through a cylindrical water filter (Pyrex, 10 Dai $\times$ 11 cm). The amount of evolved hydrogen was measured with a gas chromatograph (HP5890A) using N_2 as carrier gas.

The pore structure analysis was performed by N_2 adsorption-desorption isotherm. Surface area was determined by Langmuir and BET method.

Results and Discussion

The reflectance absorption spectra of four samples with

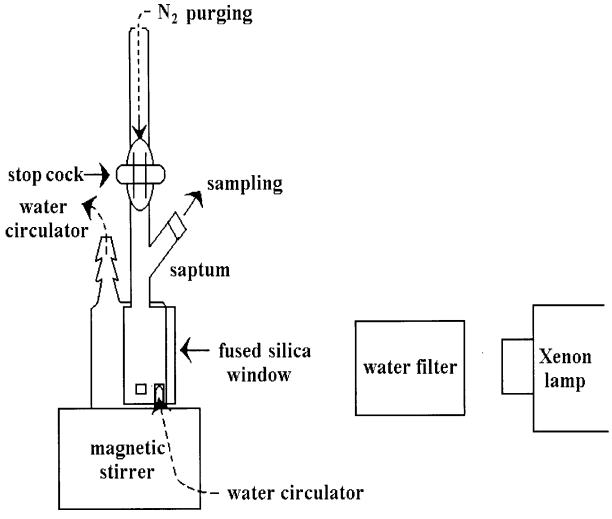

Figure 2. Schematic diagram of photoreactor.

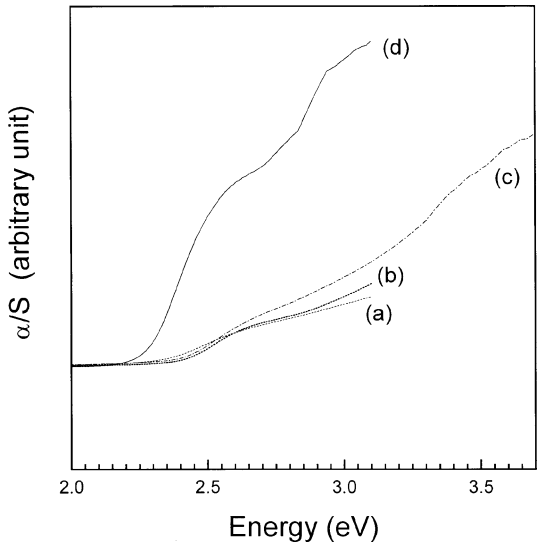

Figure 3. Absorption spectra of CdS embedded in zeolite. (a) sample A, (b) sample B, (c) sample C, (d) Bulk CdS.

different conditions for Pt and CdS loading are shown in Figure 3. UV absorption edges of samples A, B and C show a blue shift from that of bulk (around 2.28 eV). Absorption edges of samples A, B and C are 2.31 eV, 2.40 eV, 2.39 eV, respectively (Table 1). It is known that if the size of clusters gets smaller, their optical absorption edges shift to a shorter wavelength.[10] Assuming CdS has a direct band gap, the band gaps calculated are shown in Table 1. The edges on reflectance absorption spectra of CdS embedded in zeolite were very broad, which is an indication of a wide distribution of particle sizes of CdS. Therefore, it seems that CdS formation takes place not only in zeolite Y but also on the surface of zeolite Y.

Figure 4 shows the IR spectra of samples prepared by various conditions and the spectra of bulk CdS and pristine zeolite are also shown. Characteristic vibration modes of zeolite framework in the region of 400-650 cm^{-1} are attributed to Si (Al)-O bending mode and double ring mode.[9] The IR spectra of bulk CdS shows a band at 2362 cm^{-1}. The IR band at 2362 cm^{-1} from spectra of Figure 4(b)-(e) indicates the existence of CdS clusters in zeolite. The typical vibration modes of zeolite observed in Figure 4(b)-(e) indicate that all CdS embedded samples have the building units of zeolite framework. Telbiz *et al*.[9] suggested, if CdS was prepared in zeolite Y, there would be noticeable reduction in intensities at the IR band corresponding to the zeolite framework vibration and this can be explained in terms of charge delocalizations in the framework caused by CdS formation.[9] Such a charge delocalization in zeolite is considered to reduce the force constant of hexagonal or tetragonal prisms of zeolite cages. In IR spectrum of sample A, the significantly reduced band intensities at 400-650 cm^{-1} are an indication of CdS clusters formed in zeolite framework (Figure 5). Therefore, even though there might be some CdS formed on the outside of zeolite surface, it is concluded that CdS formation takes place in the cavity of zeolite Y. For sample C, the band intensities corresponding to the zeolite framework were not reduced so much as those of sample A, which indicates less amount of CdS cluster embedded in zeolite.

The amount of hydrogen evolved with 1 mg of sample was found to be dependent on the platinization process of

Table 1. Results of band gap calculation

Samples	Band gap (eV)
CdS bulk	E_g : 2.28 eV
PtCdS-A	E_g : 2.31 eV
PtCdS-B	E_g : 2.40 eV
PtCdS-C	E_g : 2.39 eV

$\alpha h\nu = \text{const}\ (h\nu - E_g)^{0.5}$ (for direct transition semiconductor)

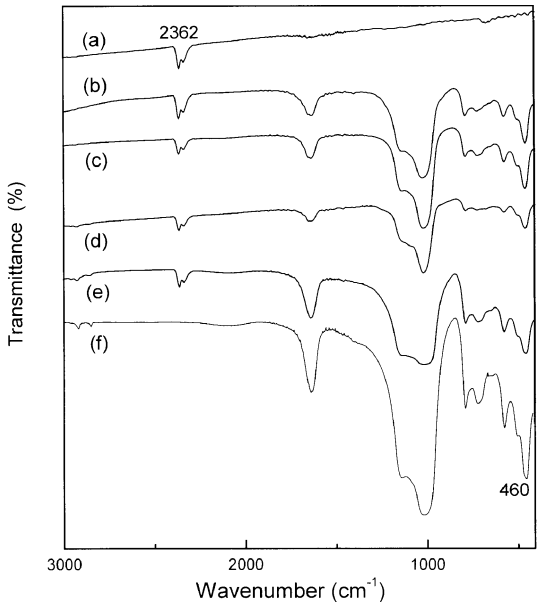

Figure 4. IR spectra of bulk CdS (a), CdS-H_2S (b), CdS-Na_2S(c), sample A (d), sample C (e) and zeolite Y(f).

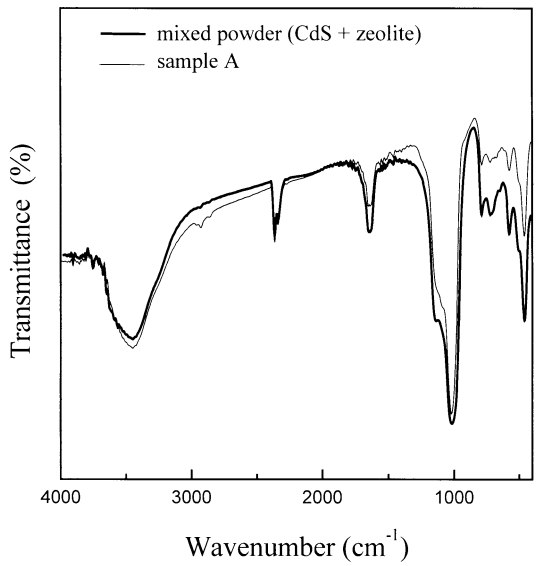

Figure 5. IR spectra of mixed powder (CdS + zeolite) (a) and sample A (b) for comparison.

Table 2. Hydrogen evolution [μL] per 1 mg of CdS in 0.1M sodium tartrate solution buffered to pH 4.1

Time(h)	PtCdS-A	PtCdS-B	PtCdS-C	CdS-Na_2S
1	1	2	12	2
2	6	8	34	4
3	17	19	49	7
4	31	32	62	9

the sample (Table 2). Even though the detailed catalytic mechanism of Pt on hydrogen evolution is not apparent, sample C appears to be more effective than the others and shows significantly improved activity (Figure 6). Even though sample A and B contain larger quantities of Pt than sample C, sample A and B show lower activities than sample C. The optimum level of Pt loading seems to be around 1 wt %.

Even though the total amounts of Pt added in the exchange reactions were the same for sample A and B (10-wt% of zeolite), the amount of Pt added at each consecutive step was different. The results of the ICP analysis show that the total amounts of Pt incorporated in sample A and B are in a range of 5-7 wt% of zeolite (Table 3). The results of ICP analysis show that the content of Pt for sample A (6.4 wt%) is slightly higher than that of sample B (5.7 wt%). For sample C, relatively small amount of Pt (0.003 g/1 g of zeolite) was incorporated at each step and the ICP analysis shows that the total amount of Pt actually incorporated is about 1 wt% of zeolite, which is the amount we actually added to incorporate. Pt clusters with small sizes formed in earlier step seem to help further growing of larger Pt clusters in zeolite cage. However, too much amount of Pt precursors may form large clusters on the surface of zeolite and blocks the pore gates, thus prevent Pt clusters from growing bigger as observed in sample A and B.

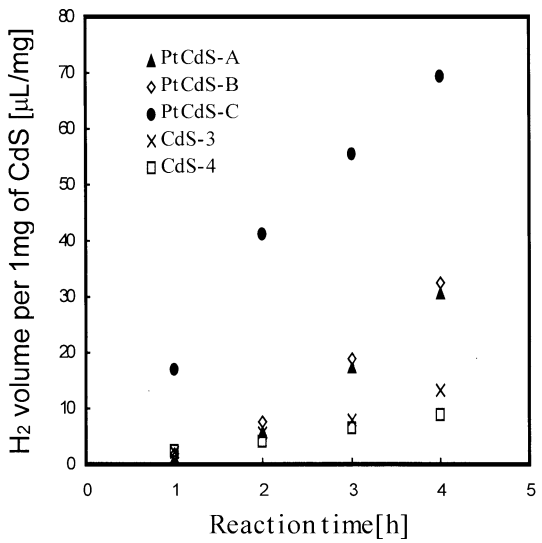

Figure 6. Hydrogen evolution [μL] per 1 mg of CdS.

Table 3. Results of elemental analysis by ICP

	Weight% of CdS and Pt in zeolite Y	
	CdS[a]	Pt
PtCdS-A	34.8	6.4
PtCdS-B	8.74	5.7
Pt CdS-C	11.3	1.07
CdS-Na_2S	13.4	
CdS-thiourea	2.3	
CdS-H_2S	1.7	

[a]The atomic ratio (Cd/S) is assumed to be 1.

Studies on the Pt supported zeolite Y (Pt/NaY) have shown that the size and the location of Pt cluster in zeolite are sensitive to supporting methods (e.g., ion exchange and impregnation) and also activation and reduction conditions.[20-26] Pandya *et al*.[27] determined the fraction of Pt quantity inside and outside of the zeolite cages by Xe NMR technique: for the sample reduced at 573 K, almost all Pt particles are located inside the zeolite supercages, while for the sample reduced at above 923 K, almost 100% of Pt clusters are located outside the zeolite framework. Tzou *et al*.[27(b)] also observed the same results about the location of Pt clusters in zeolite from EXAFS data. Therefore, to incorporate Pt clusters in zeolite Y, hopefully in supercage, ion-exchanged samples were activated at 593 K and reduced at 573 K as previous works.[20-24] We found that the platinization of CdS embedded zeolite significantly improves the efficiency of hydrogen evolution. After 4 hour reaction, 62 mL of hydrogen evolution per mg CdS in sample C (the most effective) and 9 mL/mg for Pt-loaded sample CdS-Na_2S were observed. The rate of hydrogen evolution of Pt-loaded sample C was increased about 6 times of that of Pt-unloaded sample CdS-Na_2S. But, this enhanced rate in hydrogen evolution is about 4 times slower than that reported by Fox and Pettit.[19] They observed also that Pt-loaded samples has 8-20 times enhancement in the hydrogen evolution rate. In their study, Pt clusters were grown by photoreduction of Pt $(NH_3)_4^{2+}$ with CdS, in their sample, the Pt particles seem to be located closer to CdS particles. Also, they used S^{2-}/SO_3^{2-} combination as a hole scavenger material to prevent photo corrosion of the semiconductor. However, we chose tartrate as an alternative convenient hole scavenger. The hole scavenging mechanism with tartrate is proposed as follows.[32]

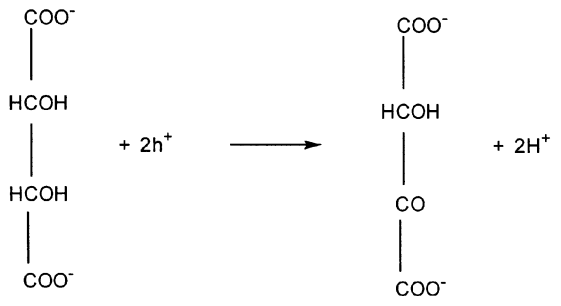

The pore volume and surface area of various samples were measured by BET method. These were determined by analyzing the nitrogen adsorption-desorption isotherm and are

Table 4. Results of pore-structure analysis

	Pore Volume (mL/g)		Surface Area (m^2/g)		
	Micro Porevolume	Total Pore Volume	by BET 0-0.1 (P/Po)	by BET 0-0.3 (P/Po)	by Langmuir
Zeolite Y	0.308019	0.337246	786	628	883
PtCdS-A	0.100174	0.252161	336	303	406
PtCdS-B	0.164296	0.287742	463	392	536
PtCdS-C	0.199209	0.289289	540	450	606
CdS-Na_2S	0.268262	0.303212	693	568	782
CdS-H_2S	0.08277	0.227409	526	426	590
CdS-thiourea	0.206517	0.21658	516	433	582

summarized in Table 4. Also, the results from the Langmuir method, which is known to give reliable information about surface area of zeolite materials, are listed for comparison.[33]

As shown in Figure 7, the adsorbed gas in zeolite Y increases abruptly at the beginning, which is due to the regularly dispersed microporous network such as supercages and sodalite cages in zeolite. We found that the surface area of sample A decreased so much comparing to that of pristine zeolite Y and other Pt supported samples. From this significant decrease in the surface area and the result of ICP analysis, sample A is considered to have more CdS clusters in pore sites than the other samples.

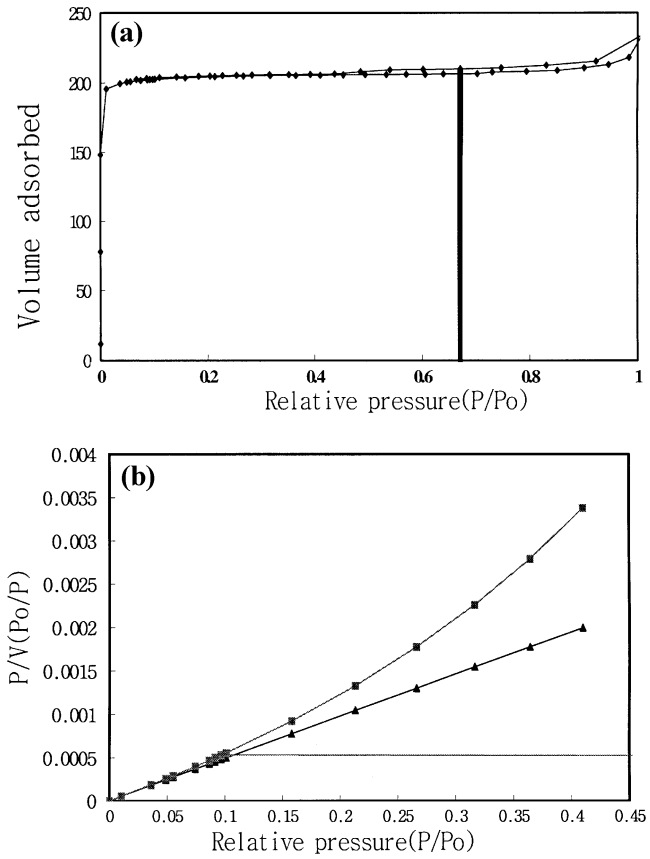

Figure 7. (a) Adsorption-desorption isotherm (inert). (b) BET and Langmuir plots

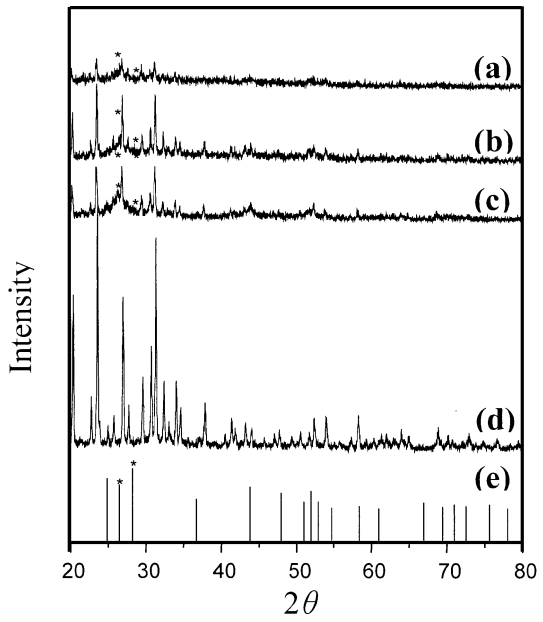

Figure 8. X-ray diffraction patterns of sample A (a), sample B (b), sample C(c), zeolite Y (d) and bulk CdS (e).

Figure 8 shows X-ray diffraction patterns of sample A, B, C, and zeolite Y, and also calculated Bragg peak positions of CdS were shown. In these XRD patterns of sample A, B, and C, the peak intensities corresponding to zeolite phase become weaker and broader peaks due to CdS phase in 25-30° (2θ) are observed. These broad diffraction peaks indicate that the size of CdS clusters is not large enough to show polycrystalline property. In XRD pattern of sample A, the peak intensities of the zeolite phase are most significantly reduced relative to the peak intensities of CdS, which indicates that sample A contains more CdS clusters in zeolite cages.

Conclusions

An integrated photocatalytic system, zeolite Y embedded with CdS and Pt, was constructed. The formation of CdS clusters in zeolite Y was confirmed by the blue shift of U.V. spectra and the relative intensity changes in IR spectra and XRD patterns. From the shape of absorption edges, it is found that CdS clusters have various size distributions suggesting CdS clusters grown not only in the cavities, but also on the outside surface of zeolite. The results of pore volume and surface area measurement indicate that the CdS formation occurs inside the zeolite cages. From the results of hydrogen evolution experiment, it is concluded that the platinization of samples significantly improves the efficiency of hydrogen evolution, however, the amount of Pt above a critical point is not an important factor for a further improved efficiency. Tartrate is found to be an effective hole scavenger in the CdS/zeolite system.

Acknowledgment. This research was supported by the fund BSRI-96-3413 and by KOSEF through the Center for Molecular Catalysis.

References

1. (a) *Energy Resources through Photochemistry and Catalysis*; Gratzel, M., Ed.; Academic Press: New York, 1983. (b) *Homogeneous and Heterogeneous Photocatalysis*; Plizzetti, E., Serpone, N., Eds.; Reidel Publishing: Dordrecht, 1986. (c) Wrighton, M. S. *Accs. Chem. Res.* **1979**, *12*, 303. (d) Wrighton, M. S. *Chem. Edu*. **1983**, *60*, 877.
2. *Solar Power and Fuels*; Bolton, J. R., Ed.; Academic Press: New York, 1977.
3. Balzani, V.; Moggi, L.; Manfrin, M. F.; Bolletta, F.; Gleria, M. *Science* **1875**, *189*, 852.
4. *Solar Radiation*; Robinson, N., Ed.; Elsevier: New York, 1966; Chapter 1.
5. *CRC Handbook of Chemistry and Physics*, 63rd ed.; Weast, R. C., Ed.; CRC Press Inc.: Boca Raton, Fl, 1982-1983; p 99.
6. Chen, W.; Wang, Z.; Lin, L. *J. Luminescence* **1997**, *71*, 151.
7. Chen, W.; Lin, Z.; Wang, Z.; Lin, L. *Solid State Commun.* **1996**, *100*, 101.
8. Chen, W.; Lin, Z.; Wang, Z.; Qian, J.; Lin, L. *Appl. Phys. Lett.* **1996**, *68*, 1990.
9. Telbiz, G.; Shwets, A.; Gunko, V.; Stoch, J.; Tamulajtis, G.; Kukhtarev, N. *Zeolites and Related Microporous Mater.: State of the Art 1994 Studies in Surface Science and Catalysis* **1994**, *84*, 1099.
10. Herron, N.; Wang, Y.; Zddy, M. M.; Stucky, G. D.; Cox, D. E.; Moller, K.; Bein, T. *J. Am. Chem. Soc.* **1989**, *111*, 530.
11. Stucky, G. D.; Mac Dougall, J. E. *Science* **1990**, *247*, 669.
12. Gutierrez-Juarez, G.; Zelaya-Angel, G.; Alvarado-Gil, J. J.; Vargas, H.; Pastore, H. O.; Barone, J. S.; Hernandez-Velez, M.; Banos, L. *J. Chem. Soc., Faraday Trans.* **1996**, *92*(14), 2651.
13. Barnakov, Yu. A.; Ivanova, M. S.; Zvinchuk, R. A.; Obryadina, A. A.; Petranovskii, V. P.; Poborchii, V. V.; Smirnov, Yu. E.; Shchukarev, A. V.; Ulashkevich, Yu. V. *Inorg. Mater.* **1995**, *31*(6), 752.
14. Barnakov, Yu. A.; Ivanova, M. S.; Zvinchuk, R. A.; Obryadina, A. A.; Petranovskii, V. P.; Poborchii, V. V.; Smirnov, Yu. E.; Shchukarev, A. V.; Ulashkevich, Yu. V. *Studies in Surface Science and Catalysis* **1994**, *84*, 829.
15. Leqlise, J.; Manoli, J. M. *J. Chatalysis* **1995**, *152*, 275.
16. Leqlise, J.; Janin, A.; Lavalley, J. C.; Cornet. D. *J. Catalysis* **1988**, *114*, 388.
17. Leqlise, J.; Qotbi, M. El.; Goupil, J. M.; Cornet, D. *Catalysis Letters* **1991**, *10*, 103.
18. Leqlise, J.; Qotbi, M. El.; Cornet, D. *Collect. Czech. Chem. Commun.* **1992**, *57*, 882.
19. (a) Breck, D. W. *Zeolite Molecular Sieves*; Krieger Publishing Co.: Malabar, FL, 1984; p 100. (b) Fox, M. A.; Rettit, T. L. *Langmuir* **1989**, *5*, 1056.
20. Ko, C. M.; Ryoo, R. *Chem. Commun.* **1996**, 2467.
21. Khodakor, A.; Barbouth, N.; Berthier, Y.; Oudar, J.; Schulz, P. *J. Chem. Soc., Faraday Trans.* **1995**, *91*, 56.
22. Vaarkamp, M.; Majet, B. L.; Kappers, M. J.; Miller, J. T.; Koningsberger, D. C. *J. Phys. Chem.* **1995**, *99*, 16067.
23. Shpiro, E. S.; Jaeger, N. I.; Schulz-Ekloff, G. *Ber. Bunsenges. Phys. Chem.* **1995**, *99*, 1321.
24. Gallezot, P.; Alarcon-Diaz, A.; Dalmon, J-A.; Renouprez, A. J.; Imelik, B. J. *Catalysis* **1975**, *39*, 334.
25. Boyanov, B. I.; Morrison, T. I. *J. Phys. Chem.* **1996**, *100*, 16310.
26. Rabo, J. A.; Schomaker, V. *Proc. 3rd Int. Congr. Catal.* **1964**, *2*, 1264.
27. (a) Pandya, K. I.; Heald, S. M.; Hriljac, J. A.; Petrakis, L.; Fraissard, J. *J. Phys. Chem.* **1996**, *100*, 5070. (b) Tzou, M. S.; Teo, B. K.; Sachtler, W. M. H. *J. Phys. Chem.* **1991**, *95*, 5210.
28. Pankove, J. I. *Optical Procedd in Semiconductors*; Dover Publication: New York, 1976.
29. Dyer, A. *An Introduction to Zeolite Molecular Sieves*; John Wiley & Sons: Chichester, 1989; p 34.
30. Himei, H.; Yamadaya, M.; Oumi, Y.; Kubo, M.; Stirling, A.; Vetrivel, R.; Broclawik, E.; Miyamoto, A. *Microporous Materials* **1996**, *7*, 235.
31. Ishigoh, K.; Tanaka, K.; Zhuang, Q.; Nakata, R. *J. Phys. Chem.* **1995**, *99*, 12231.
32. Enea, O.; Bard, A. J. *J. Phys. Chem.* **1986**, *90*, 301.
33. Breck, D. W. *Zeolite Molecular Sieves*; John Wiley & Sons: New York, 1974; p 628.